Effect of the Plasma Density Scale Length on the Direction of Fast Electrons in Relativistic Laser-Solid Interactions

M. I. K. Santala,* M. Zepf, I. Watts, F. N. Beg, E. Clark, M. Tatarakis, K. Krushelnick, and A. E. Dangor
Plasma Physics Group, The Blackett Laboratory, Imperial College, London SW7 2BZ, United Kingdom

T. McCanny, I. Spencer, R. P. Singhal, and K. W. D. Ledingham
Department of Physics and Astronomy, University of Glasgow, Glasgow G12 8QQ, United Kingdom

S. C. Wilks
University of California, Lawrence Livermore National Laboratory, L-39, Livermore, California 94550

A. C. Machacek and J. S. Wark
Clarendon Laboratory, Parks Road, Oxford OX1 3PU, United Kingdom

R. Allott, R. J. Clarke, and P. A. Norreys
Central Laser Facility, Rutherford Appleton Laboratory, Chilton OX11 0QX, United Kingdom
(Received 16 February 1999; revised manuscript received 21 January 2000)

The angular distribution of bremsstrahlung γ rays produced by fast electrons accelerated in relativistic laser-solid interaction has been studied by photoneutron activation in copper. We show that the γ-ray beam moves from the target normal to the direction of the $\mathbf{k}_{\text{laser}}$ vector as the scale length is increased. Similar behavior is found also in 2D particle-in-cell simulations.

PACS numbers: 52.40.Nk, 52.25.Nr, 52.60.+h

Developments in laser technology over the past few years have made experiments at focused intensities 10^{19}–10^{20} W/cm^2 feasible. Large numbers of high energy electrons are generated in laser-solid interactions at these intensities as predicted by computer simulations [1,2] and confirmed by a number of experiments [3–6]. There are many potential mechanisms for fast electron generation, e.g., classical and Brunel-type resonance absorption [7,8], ponderomotive $\mathbf{j} \times \mathbf{B}$ acceleration [1] (possibly affected by a self-generated azimuthal magnetic field [2]), and wake-field acceleration [9,10].

The different mechanisms produce differing angular distributions of the accelerated electrons: the resonance absorption processes are expected to produce electrons mainly in the direction of the density gradient ∇n_e for p-polarized light while the other two mechanisms would produce electrons mainly in the laser beam propagation direction $\mathbf{k}_{\text{laser}}$. By studying the angular distribution of γ-ray beams, information about the fast electron generation mechanisms can be obtained. From the standpoint of many practical applications, e.g., the fast ignitor concept [11], it is important to understand the relative importance of these acceleration methods under different plasma conditions.

In this paper we have experimentally studied the angular distribution of >10 MeV electrons under different plasma scale-length conditions. The angular distributions were measured using photonuclear activation techniques previously used in resolving γ-ray spectra [12]. We also compare our experimental results to 2D particle-in-cell (PIC) simulations and find that changes in the scale length correspond to the above-mentioned changes in the principal electron-acceleration mechanism. We show that the γ-ray beam moves from the target normal to the direction of $\mathbf{k}_{\text{laser}}$ as the scale length is increased and becomes random at very large scale lengths.

The experiment was carried out using the chirped pulse amplification beam of the VULCAN Nd:glass laser system at Rutherford Appleton Laboratory (RAL) [13]. The laser wavelength was 1.054 μm, pulse length was 1–1.5 ps, and energy incident on target was 20–50 J. The laser beam (111 $\times$ 200 mm) was focused onto the target surface using a $f = 225$ mm on-axis parabolic mirror. The laser beam was p polarized and was incident on target at an angle of 45°. Intensity on target was measured by an x-ray penumbral camera, and it was typically $(1–3) \times 10^{19}$ W/cm^2.

The targets (see Fig. 1) were 1.75 mm thick, 1×1 cm^2 tantalum slabs backed by 3 mm of copper. These were surrounded by 12 copper wedges for determination of the angular distribution, each wedge covering an angle of 10°. The wedges were 10 mm in the radial direction, 15 mm high, and 2.5 mm thick at midpoint.

Because of its high Z (73), the tantalum slab is efficient in converting kinetic energy of the fast electrons into high energy bremsstrahlung γ rays. These γ rays can then induce photoneutron reactions $^{63}\text{Cu}(\gamma, n)^{62}\text{Cu}$ in the surrounding copper. This reaction has a threshold of about 10 MeV and the cross section reaches about 70 mb (1 mb $= 10^{-31}$ m^2) at 17 MeV [14,15]. The resulting ^{62}Cu isotope has a 9.74 min half-life, and it is a nearly pure ($>99\%$) β^+ emitter [16]. This allows highly sensitive

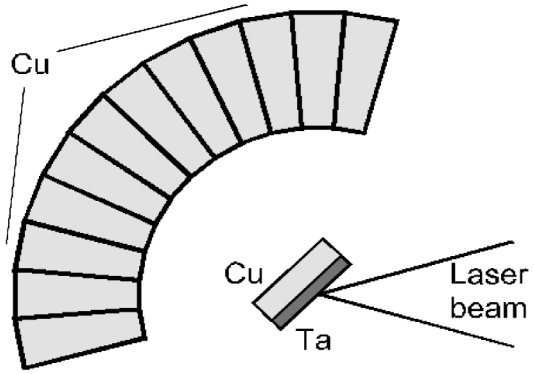

FIG. 1. Schematic drawing of the target setup.

detection of low levels of activation by using coincidence techniques for detecting the 511 keV annihilation γ's [17]. The setup used has two 3 in. $\times$ 3 in. NaI(Tl) scintillators yielding about 14% detection efficiency and a detection threshold of about 0.2 Bq [1 Bq (becquerel) = one nuclear disintegration per second].

The copper slab directly behind the tantalum slab acted as an overall activation reference. The angular distribution of the bremsstrahlung is found by measuring the activation in each of the wedged copper pieces surrounding the target. Simulations of bremsstrahlung generation by GEANT Monte Carlo code [18] show that the direction of high energy bremsstrahlung closely matches that of the incident electrons. Exponential electron distributions with temperatures between 1.5 and 10 MeV incident on 3 mm lead is found to produce bremsstrahlung above 10 MeV in a 10°–12° (FWHM) cone. Thus the activation distribution gives a good approximation of the angular distribution of fast electrons.

The main laser pulse is always preceded by a low intensity, long duration pedestal (300 ps through 1 ns) produced by amplified spontaneous emission and from imperfect compression of the chirped pulse. This has sufficient intensity to produce a preplasma in front of the solid interface. As the critical surface moves away from the ablation front, the main laser-plasma interaction takes place in this preplasma. It appears from our measurements that the density scale length of the preplasma affects the interaction physics significantly.

The density scale length can be changed by adjusting the duration of the pedestal preceding the main pulse. This was accomplished by altering the timing of optical gates in the laser chain. A temporally short pedestal results in a preplasma that has little time to expand and thus a small scale length. Very large scale lengths were obtained by deliberately introducing a prepulse before the main pulse.

The size of preplasma was measured by taking a shadowgraphic image of the target surface 30 ps before the main laser pulse (see Refs. [19,20]). A 10 ps, 2ω laser beam was used for back-illumination, and the target was imaged onto a charge-coupled device. The distance from the ablation front to the edge of the inaccessible region (δ) was measured from the images. This is a measurement of refraction of light in plasma and is essentially an integral of transverse density gradient along the beam path. The inaccessible region results from refraction of light out of the collection optics. The accuracy of this measurement is estimated to be about ± 15 μm, mainly due to errors in determining the position of the ablation front in the shadowgrams.

A first-order estimate for plasma density scale-length (L) can be calculated from the measured δ. Assuming an exponential electron density profile $n_e(x) = n_{e,0}\exp(-x/L)$, and $n_{e,0} = 1.0 \times 10^{24}$ cm^{-3} ([Xe]-like Ta) it can be shown that the edge of inaccessible region $\delta = 9L$. The estimate is not very sensitive to the exact value of $n_{e,0}$. The scale lengths in this paper have been calculated using this simple model. Extensive computer simulations would be needed to yield a more accurate estimate.

In total, simultaneous angular distributions and scale-length data were collected on 17 shots. Most of the shots were with a relatively small prepulse resulting in a plasma scale length $L < 10$ μm. On three shots a very large preplasma was created by a prepulse having 6% of laser energy which preceded the main pulse by 0.3–1.5 ns.

The measured activation angular distributions were corrected for decay and scaled to give relative peak flux of 1. By fitting a Gaussian distribution an estimate for the main beam direction was found. The fitting error is typically less than 1°. The main error source is the positioning accuracy of the laser beam on target surface which is estimated to be within a $r = 1$ mm circle. This gives a peak angular error of $\pm 3°$.

Figure 2 displays angular spectra obtained in the large L (Fig. 2a) and the intermediate L (Fig. 2b) cases. The width of these distributions is 35–40° (FWHM). Very wide (Fig. 2c, width = 56°) or double-peaked (Fig. 2d)

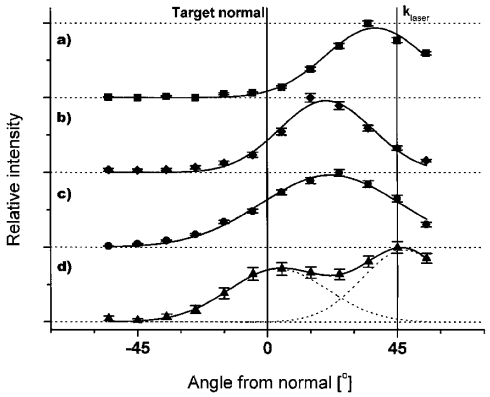

FIG. 2. Four normalized angular distributions fitted with Gaussian distributions, offset for clarity. (a) Large scale length ($L = 5.9$ μm) and (b) small scale length ($L = 2.6$ μm) cases. (c) and (d) show evidence of two different beams as a very wide single peak (c) and as a double-peaked distribution (d).

distributions were sometimes observed. This can be seen as evidence of generation of two separate electron beams that generate two partially overlapping γ-ray beams.

To find if there is correlation between the plasma scale length and the direction of main γ-ray emission, the peak of γ-ray emission is plotted against measured size of preplasma in Fig. 3. It can be observed that these two are linearly correlated ($r^2 = 0.81$) for L less than about 10 μm. However, at very large L (obtained with large prepulse) no correlation is observed.

The observed correlation between L and electron angular distribution could be explained by Brunel-type resonance absorption being the dominant absorption mechanism in plasmas with a steep density gradient ($L \approx \lambda$). As the plasma scale length increases, the $\mathbf{j} \times \mathbf{B}$ type mechanism becomes the main hot electron production mechanism. This simple picture breaks down at shallow density gradients ($L \gg \lambda$). The converging laser beam has to traverse a large distance in coronal plasma which results in an essentially random angular distribution. This may be due to filamentation and self-focusing of the laser beam in the underdense plasma [21] or, e.g., hosing instability [22].

The absolute activation in the reference copper piece showed large shot-to-shot variations. The initial activity ranged from 4 to 1400 Bq. The average was 300 Bq, standard deviation of 330 Bq, and median 190 Bq. Below 10^{18} W/cm^2 there was little activation but otherwise there was no correlation with intensity. The activation yield showed no correlation to plasma scale length either suggesting that the different mechanisms have similar efficiency of fast electron production. However, even if there was a correlation it might be lost in practice as only the electrons far in the tail of distribution can produce γ rays with a sufficient energy to induce activation.

The γ-ray generation was simulated using the GEANT code. Electrons which had an exponential energy distribution were incident on 3 mm thick lead target (i.e., having a similar areal density as the tantalum target). The γ-ray spectra were folded with the (γ, n) reaction cross section. For electron temperatures 1.5, 2.5, and 4 MeV activities 7.6, 250, and 2200 Bq/J (energy in total electron distribution), respectively, were obtained in a 3 mm thick copper piece. Thus small shot-to-shot variations in temperature result in such large variations in activation that they can mask any correlations. These variations make it difficult to estimate the fast electron yield precisely without a corresponding angularly resolved temperature measurement for each shot. Therefore the determination of the fast electron production efficiency will be the subject of further investigation.

We have carried out 2D PIC simulations using the ZOHAR code [1] to study the angular properties of fast electron generation. Results for a p-polarized laser beam incident to a $8n_c$ plasma slab at 40° off-normal angle taken after 15 laser cycles are shown in Fig. 4. Plotted here is the electron phase space for electrons with energies greater than 1 MeV directed into the target. The threshold for copper activation corresponds to radius $20p/m_0c$ in the figure.

It is evident that when the laser beam is incident to a steep density gradient (Fig. 4a), the electrons are mainly directed near the target normal direction ($p_y \approx 0$). When the scale length is increased (Fig. 4b) an additional electron beam is generated in the direction of laser beam propagation ($p_y \approx p_x$). This suggests a change in the relative importance of different fast electron generation mechanisms in larger scale-length plasmas, in an agreement with our experimental observations and the discussion above.

The simulated intensity (10^{20} W/cm^2), while higher than measured in our experiment, illustrates the essential physics. The simulations were also run at lower intensity and showed qualitatively similar behavior. However, the number of high energy electrons is too small to explain the observed activation. This may be an indication of a significant relativistic self-focusing under our experimental conditions.

Another mechanism which could contribute to the observed behavior of the γ-ray beam results from the expansion of the preplasma and the motion of

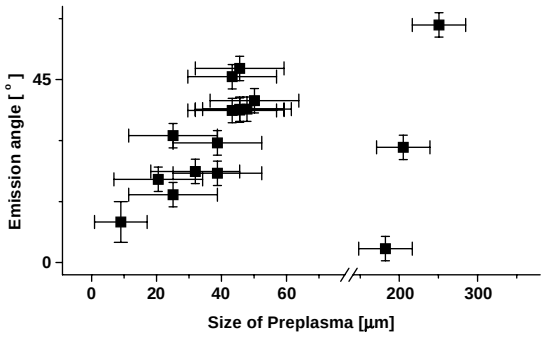

FIG. 3. The direction of the main γ-ray emission vs the size of preplasma (the distance δ from the ablation front to the edge of the inaccessible region). For exponential density profile plasma scale length $L = \delta/9$.

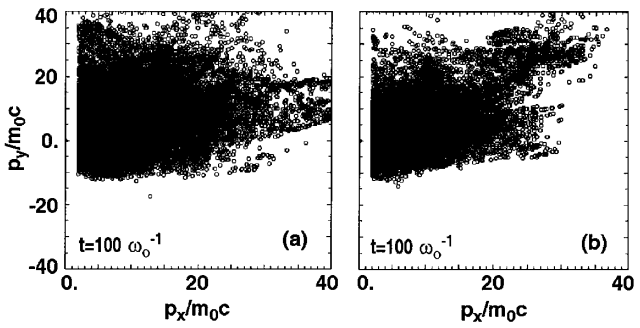

FIG. 4. PIC simulation results of electron momentum distributions at 10^{20} W/cm^2. A p-polarized laser beam is incident at 40° off-normal angle to a sharp density gradient (left) or to a finite scale-length plasma of $L = 0.5$ μm.

the critical density surface with it. If the stand-off distance between the critical density surface and the ablation front is comparable to the focal spot size or is larger, then it is possible that the critical surface is not parallel to the target surface (and possibly is not even planar). Consequently, the main interaction could take place at an angle smaller than the original 45°. The observation of two separate beams, one at 0° and another at 45°, shows, however, that this mechanism is not sufficient to explain our results.

The experimental data show some shot-to-shot variations in the observed emission angles and, in particular, the width of emission. This behavior could be taken as evidence of variations caused by motion of critical surface. As the critical surface becomes perpendicular to $\mathbf{k}_{\text{laser}}$ the electron beams generated by the different mechanisms will be more parallel to each other. It then becomes more likely that magnetic interaction between the electron beams can change their direction of propagation.

Fields in excess of 500 T have been predicted in the solid over distances of tens of micrometers due to current of fast electrons [23]. In the interaction region even higher fields exceeding 10^4 T are predicted [24,25]. The Larmor radius $r_{\text{L}} = p/qB$ of a 10 MeV electron in 500 T field is about 65 μm and in 10^4 T field only 3.3 μm. Depending on the structure of the fields it appears likely that the fast electrons can change their direction while traversing such fields or that two beams could coalesce altogether. If the electron beams and corresponding fields are weak, they could be only slightly bent resulting in a double-peaked emission or in a wide emission peak. If only one beam is dominant, a fairly narrow emission would be observed but possibly in a direction differing from that of the original beam. Another weaker beam could manifest itself as an additional "bump" or increased tail in the emission. These structures were often observed in the angular distributions, but they may not always be statistically significant.

It should be emphasized that the presently used method of photoneutron reactions in copper is sensitive to electrons only above 10 MeV. It cannot provide direct information about the electrons at lower energy, which may affect the magnetic fields generated. However, the fastest electrons are more likely to convey the information about the original beam direction as the r_{L} scales nearly linearly with energy for multi-MeV electrons. The self-generated fields are thus able to affect the low energy electrons more easily. By using other elements for detection of energetic electrons via nuclear activation the threshold could be varied from 7 to 20 MeV [26].

In conclusion, we have shown a correlation between the plasma density scale length L and the main direction of fast (>10 MeV) electron generation using photoneutron reactions in copper. That is to say, for very small $L < \lambda$ the γ-ray beam is normal to the target, for intermediate $L \approx 5\lambda$ the beam is along $\mathbf{k}_{\text{laser}}$, and for long $L \gg \lambda$ the beam direction is uncorrelated. The photoneutron activation techniques used have been found to be powerful diagnostic tools in highly relativistic laser-plasma experiments.

The authors acknowledge the excellent support of all the laser engineering and target area staff of the Central Laser Facility. This work was supported by EPSRC grants (No. GR/K93815 and No. GR/L04498), and M. S. was supported by EU TMR network SILASI (No. ERBFMRX-CT96-0043) and the Jenny and Antti Wihuri Foundation.

*Present address: Helsinki University of Technology, P.O. Box 2200, 02015 HUT, Finland.

[1] S. C. Wilks *et al.*, Phys. Rev. Lett. **69**, 1383 (1992).
[2] A. Pukhov and J. Meyer-ter-Vehn, Phys. Plasmas **5**, 1880 (1998).
[3] G. Malka and J. L. Miquel, Phys. Rev. Lett. **77**, 75 (1996).
[4] T. Feurer *et al.*, Phys. Rev. E **56**, 4608 (1997).
[5] G. Malka, E. Lefebvre, and J. L. Miquel, Phys. Rev. Lett. **78**, 3314 (1997).
[6] K. B. Wharton *et al.*, Phys. Rev. Lett. **81**, 822 (1998).
[7] F. Brunel, Phys. Rev. Lett. **59**, 52 (1987).
[8] S. C. Wilks and W. L. Kruer, IEEE J. Quantum Electron. **33**, 1954 (1997).
[9] T. Tajima and J. M. Dawson, Phys. Rev. Lett. **43**, 267 (1979).
[10] F. Amiranoff *et al.*, Phys. Rev. Lett. **81**, 995 (1998).
[11] M. Tabak *et al.*, Phys. Plasmas **1**, 1626 (1994).
[12] M. H. Key *et al.*, Phys. Plasmas **5**, 1966 (1998).
[13] C. N. Danson *et al.*, J. Mod. Opt. **45**, 1653 (1998).
[14] B. L. Berman and S. C. Fultz, Rev. Mod. Phys. **47**, 713 (1975).
[15] EXFOR on-line database at http://www-nds.iaea.org
[16] NUDAT on-line database at http://www-nds.iaea.org
[17] G. F. Knoll, *Radiation Detection and Measurement* (Wiley, New York, 1989), 2nd ed.
[18] CERN Program Library Long Writeup W5013.
[19] M. Tatarakis *et al.*, Phys. Rev. Lett. **81**, 999 (1998).
[20] P. Norreys *et al.*, Phys. Plasma **6**, 2150 (1999).
[21] C. E. Max, J. Arons, and A. B. Langdon, Phys. Rev. Lett. **33**, 209 (1974).
[22] K. C. Tzeng *et al.*, Phys. Plasma **6**, 2105 (1999).
[23] J. Davies, A. R. Bell, and M. Tatarakis, Phys. Rev. E **59**, 6032 (1999).
[24] A. Pukhov and J. Meyer-ter-Vehn, Phys. Rev. Lett. **76**, 3975 (1996).
[25] R. J. Mason and M. Tabak, Phys. Rev. Lett. **80**, 524 (1998).
[26] K. W. D. Ledingham *et al.*, Phys. Rev. Lett. **84**, 899 (2000).